焊剂带约束电弧在超窄间隙焊接中的加热特性

郑韶先， 朱 亮， 张旭磊， 陈剑虹
（兰州理工大学 甘肃省有色金属新材料省部共建国家重点实验室，兰州 730050）

摘 要：利用焊剂带约束的电弧进行超窄间隙焊接，通过测量不同焊接参数下的焊缝截面相关尺寸，并根据截面尺寸的变化规律分析了受约束电弧的加热特性。结果表明，对超窄间隙中的电弧加以有效约束，有利于防止电弧攀升，并能保证两侧壁可靠熔合；电弧形态是决定侧壁熔合的主要因素，增加焊接电流或送带速度，可使电弧的加热位置下移，电弧直接加热侧壁的高度减小，以至电弧能量密度提高，更有利于电弧对侧壁根部的加热；增加电弧电压，可使阴极斑点的活动范围增加，有利于增强弧柱和阴极斑点对侧壁根部的加热效果；电弧电压、焊接电流和送带速度三者间的合理匹配，有利于获得合适的电弧形态，使电弧在间隙的三个方向有效加热。

关键词：焊剂带约束电弧；超窄间隙焊接；加热特性
中图分类号：TG444.7 文献标识码：A 文章编号：0253－360X(2008)05－0057－05

郑韶先

0 序 言

与常规窄间隙焊接技术相比，超窄间隙焊接更加节能省材，生产效率显著提高，焊接热输入大大降低，特别是在细晶粒钢的焊接方面，超窄间隙焊接表现出了显著的优越性和广阔的应用前景[1,2]。然而，超窄间隙焊接却存在电弧易沿间隙侧壁攀升的问题，为此通过采用焊剂片约束电弧和焊剂带约束电弧的方法进行了超窄间隙焊接，取得了良好的焊接效果[3,4]；另外，文献[5]也提出了一种超窄间隙焊接方法，该方法通过控制脉冲电弧使焊丝伸出长度发生周期性地改变，从而使电弧沿间隙侧壁上下运动。但试验结果表明，该方法虽然能够使电弧不发生攀升，却不能使电弧有效加热间隙底部，以至上下两道焊缝交接处不易熔合。

位于超窄间隙中的电弧当受到焊剂带的不同约束时，它对间隙两侧壁及其底部的加热效果不同，因而母材熔化区的形状和尺寸也不同，通过测量不同参数下的超窄间隙焊缝截面相关尺寸，并根据焊缝截面尺寸的变化规律，可对超窄间隙中焊剂带约束电弧的加热特性进行分析。从保证电弧对间隙底部，尤其是侧壁根部的有效加热考虑，有必要深入认识超窄间隙中焊剂带约束电弧对间隙两侧壁及其底部的加热特性，以及受到约束电弧加热后两侧壁及其底部的熔化特性，从而为进一步利用焊剂带调控电弧以提高超窄间隙焊接过程的稳定性提供理论依据，并有利于尽快实现焊剂带约束电弧超窄间隙焊接的工业化应用。

利用电弧电压、焊接电流、送带速度对焊缝截面尺寸的影响，分析了超窄间隙中焊剂带约束电弧的加热特性。

收稿日期：2007－06－20
基金项目：国家自然科学基金资助项目(50775105)；兰州理工大学博士基金(SB01200702)；中国机械工程学会焊接学会创新思路预研经费资助项目(07－12－005)

1 试验方法

如图 1 所示，在电弧引燃的同时，两条由焊剂制成的焊剂带紧贴间隙侧壁被连续送入电弧两侧，由于焊剂带的绝缘作用，电弧被约束在间隙底部的一

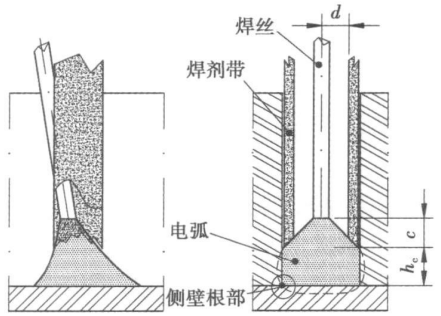

图 1 焊剂带约束电弧超窄间隙焊接示意图

Fig. 1 Schematic diagram of ultra－narrow gap welding with flux strips constricting arc

定范围内燃烧，通过增加送带速度可进一步提高焊剂带对电弧的约束程度，使电弧有效加热两侧壁及其根部，电弧和熔池则主要利用氩气进行保护。焊剂带是将焊剂压涂在薄钢带两表面而制得，其宽度为6 mm，厚度为0.5 mm，薄钢带的厚度为0.1 mm。试验所用焊接电源为平特性，采用反极性焊接，焊丝为H08Mn2Si，工件材料为低碳钢，试验所用焊接工艺参数见表1。

表1 焊接工艺参数

Table 1 Welding parameters

电弧电压 U/V	焊接电流 I/A	间隙宽度 G_w/mm	送丝速度 v_f/(mm·s^{-1})	焊接速度 v/(mm·s^{-1})	送带速度 v_d/(mm·s^{-1})	气体流量 q/(L·min^{-1})
20～23	220～270	5	48～64	8.3	7.3～15.7	10

超窄间隙焊接的根本目的是为了保证侧壁熔合良好，它不仅包括两侧壁的熔合，而且还包括间隙底部的熔合，因而超窄间隙焊接时，电弧必须同时对两侧壁和间隙底部有效加热。为了便于描述电弧对侧壁和间隙底部的加热效果，以反映电弧对侧壁和间隙底部的加热特性，对超窄间隙焊缝横截面的相关几何尺寸做了如下定义。如图2所示，G_w 为间隙宽度，h_d 为侧壁熔深，B_1 为底部熔宽，h_m 为侧壁熔高，h_b 为底部熔深，其中底部熔宽 B_1 是最为关键的尺寸，保证侧壁熔合良好的前提条件就是 $B_1 > G_w$。电弧对两侧壁及焊道底部的加热能力越强，h_d，h_b 及 B_1 的值就越大，侧壁熔合也就越好。

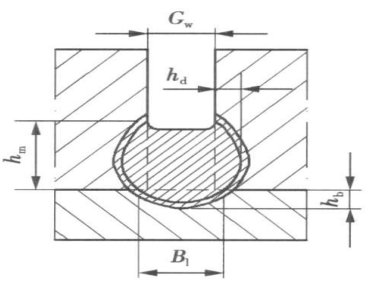

图2 超窄间隙焊缝截面尺寸示意图

Fig. 2 Schematic diagram of cross sectional size of ultra—narrow gap welds

2 试验结果及分析

2.1 超窄间隙焊缝形貌

图3为电弧受焊剂带约束的超窄间隙焊缝截面形貌，可以看出间隙两侧壁及其底部熔合良好，焊缝内部无宏观缺陷，单道焊缝的高度与间隙宽度相当，约为5 mm。

2.2 焊接参数对超窄间隙焊缝截面尺寸的影响

电弧电压决定着超窄间隙焊接电弧能否加热到两侧壁，而电弧对两侧壁和间隙底部加热作用的强弱则取决于焊接电流，只有在合适的送带速度范围内电弧才能被有效约束，从而使电弧加热位置下移以确保侧壁根部被可靠熔化。

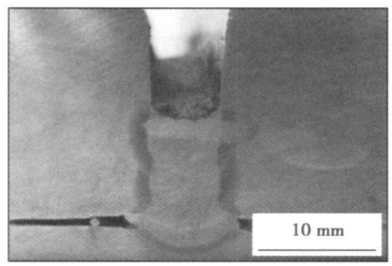

图3 焊剂带约束电弧超窄间隙焊缝形貌

Fig. 3 Morphology of ultra—narrow gap welds with flux strip constricting arc

图4为电弧电压对超窄间隙焊缝横截面尺寸的影响，所用焊接电流为240 A，送带速度为13.5 mm/s。可以看出，增加电弧电压，侧壁熔高和底部熔宽有明显增加，但底部熔深略有减小，侧壁熔深略有增加。如图1所示，在其它焊接参数确定的情况下，电弧电压增加，电弧弧柱的长度和高温区宽度将显著增加，从而使焊剂带作用长度 c 变短，电弧直接加热侧壁的高度 h_c 增加，因此焊缝的侧壁熔高明显增加；同时，电弧阴极斑点的活动范围将扩大，这在电弧不攀升的情况下有利于阴极斑点对侧壁根部的加热，因而底部熔宽明显增加。另外，电弧阴极斑点活动范围的增大，使得电弧弧柱的电流密度减小，因而流经间隙底部的电流减小，流经两侧壁的电流增加，但由于流经两侧壁和间隙底部的电流变化范围较小，所以侧壁熔深略有增加而底部熔深略有减小。

图5为焊接电流对超窄间隙焊缝横截面尺寸的影响，所用电弧电压为21 V，送带速度为13.5 mm/s。可以看出，随着焊接电流的增加，侧壁熔高和底部熔宽明显增加，但侧壁熔深略有减小，底部熔深略有增

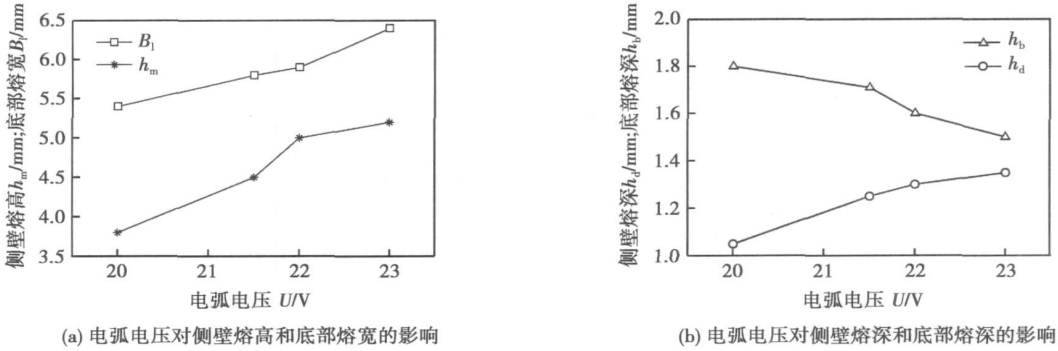

(a) 电弧电压对侧壁熔高和底部熔宽的影响　　(b) 电弧电压对侧壁熔深和底部熔深的影响

图 4　电弧电压对超窄间隙焊缝横截面尺寸的影响

Fig. 4　Influence of voltage on size of cross section of ultra— narrow gap welds

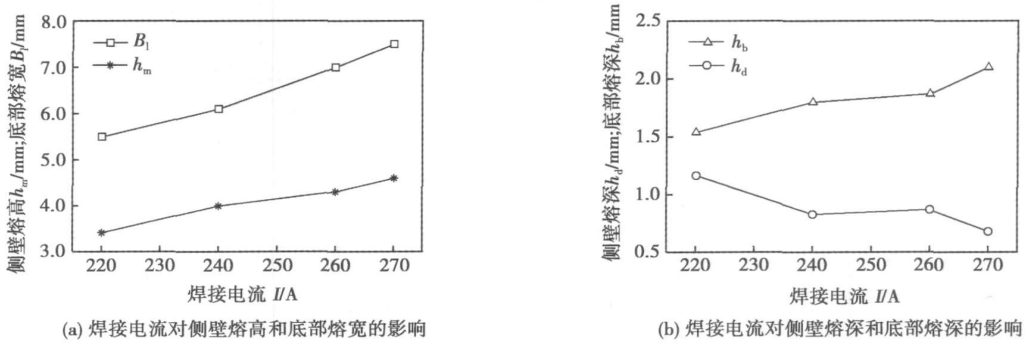

(a) 焊接电流对侧壁熔高和底部熔宽的影响　　(b) 焊接电流对侧壁熔深和底部熔深的影响

图 5　焊接电流对焊缝横截面尺寸的影响

Fig. 5　Influence of current on size of cross section of welds

加。在其它焊接参数确定的情况下，焊接电流增加，送丝速度也相应成比例增加，因而熔化的焊丝在间隙中的填充高度是增加的，所以侧壁熔高也相应增加。另外，如图 1 所示，焊接电流增加，电弧的弧柱长度变短，电弧加热更集中，因而电弧直接加热侧壁的高度 h_c 将减小，以至流经两侧壁的电流减小，流经间隙底部的电流增加，但由于电弧弧柱的电流密度提高，所以流经两侧壁的电流变化不大，侧壁熔深略有减小，而流经间隙底部的电流增加较大，只是由于熔池体积的逐渐增大，使电弧阴极斑点主要集中在熔池表面加热，因而阴极斑点对间隙底部的直接加热作用减弱，致使底部熔深略有增加。只有在熔池的前部，熔化金属较少，电弧阴极斑点可以直接有效加热两侧壁根部，所以底部熔宽明显增加。

图 6 为送带速度对超窄间隙焊缝横截面尺寸的影响，所用电弧电压为21 V，焊接电流为240 A。可以

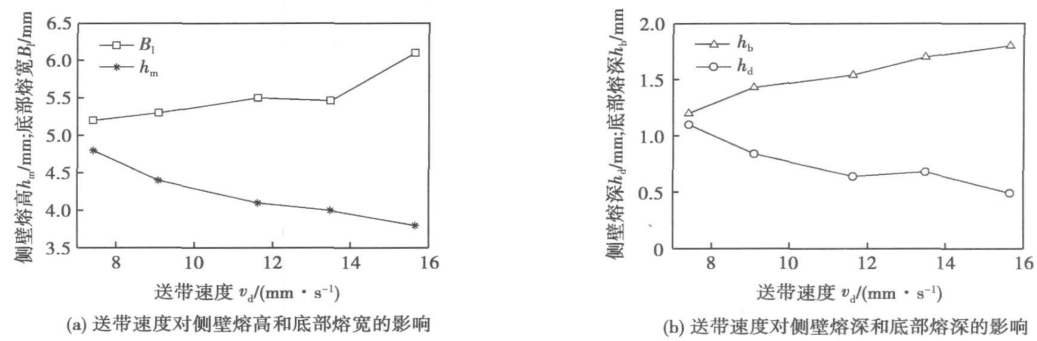

(a) 送带速度对侧壁熔高和底部熔宽的影响　　(b) 送带速度对侧壁熔深和底部熔深的影响

图 6　送带速度对焊缝横截面尺寸的影响

Fig. 6　Influence of feeding rate flux strip on size of cross section of welds

看出，增加送带速度，侧壁熔高明显减小，底部熔宽明显增加，但侧壁熔深略有减小，底部熔深略有增加。如图 1 所示，在其它焊接参数确定的情况下，送带速度增加，使得焊剂带作用长度 c 增长，电弧直接加热侧壁的高度 h_c 减小，所以电弧阴极斑点被约束在更小的范围内以利于加热两侧壁根部，因而侧壁熔高明显减小，底部熔宽明显增加；同时，由于电弧阴极斑点被约束在更小的范围内，所以弧柱的电流密度提高，以至流经两侧壁的电流减少，而流经间隙底部的电流相应增加，但流经两侧壁和间隙底部的电流变化范围较小，因而侧壁熔深略有减小，底部熔深略有增加。

上述电弧电压、焊接电流、送带速度对超窄间隙焊缝截面尺寸的影响分析表明，电弧形态是决定侧壁熔合的主要因素。如图 1 所示，通过调节焊接工艺参数，可使电弧的加热位置下移，电弧直接加热侧壁的高度 h_c 减小，以至电弧能量密度提高，更有利于电弧对侧壁根部的加热，增加焊接电流和送带速度便属于这种情况。但增加电流将使电弧的输出热和电弧力都提高，而增加送带速度不仅没能使电弧的输出热增加，反而要消耗部分电弧热以熔化焊剂带。因而由图 5 和图 6 可以看出，增加焊接电流要比增加送带速度更有利于底部熔宽 B_1 的增大；通过增加电弧阴极斑点的活动范围，也有利于弧柱和阴极斑点对侧壁根部的加热，增加电弧电压便属于这种情况。可见，焊接参数达到合理的匹配，尤其是电弧电压、焊接电流和送带速度三者间的匹配，有利于获得合适的电弧形态，使电弧在间隙三个方向有效加热，这是保证约束电弧和侧壁熔合良好的关键。

3 讨 论

侧壁根部不易被电弧加热是窄间隙焊接侧壁熔合不良的主要原因[4]，为了保证侧壁的可靠熔合并尽量降低焊接时的热输入，采用超窄间隙焊接是一种行之有效的解决方法[3]。然而，超窄间隙焊接时电弧易发生攀升，所以防止电弧攀升是进行超窄间隙焊接的关键。图 7 为文献[5]通过控制脉冲电弧使其沿间隙侧壁上下运动获得的超窄间隙焊缝截面形貌，可以看出在上下两道焊缝交接处明显未熔合，单道焊缝的高度明显大于间隙宽度，约为9 mm，并且在第一道焊缝内部存在裂纹。上述结果表明，通过控制脉冲电弧使其沿间隙侧壁上下运动的方法尽管能够防止电弧发生攀升，但由于电弧未受到约束，因而电弧阴极斑点较发散，并易集中分布于间隙两侧壁，以至电弧加热区高度明显大于间隙宽度，这是导致上下两道焊缝交接处不易熔合的主要原因。可见，在超窄间隙侧壁两侧对电弧加以适当约束，可使阴极斑点的加热位置下移至间隙底部，同时电弧能量密度获得提高，从而有利于增强电弧对间隙底部，尤其是侧壁根部的加热，因而可得到尽量大的底部熔宽 B_1，这是焊剂带约束电弧超窄间隙焊接方法能够防止电弧攀升，并保证电弧在间隙三个方向有效加热的主要原因。

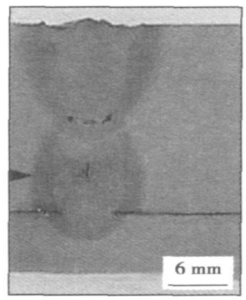

图 7 电弧沿侧壁上下运动所获得的超窄间隙焊缝形貌

Fig. 7 Morphology of ultra－narrow gap welds obtained by arc moving along the sidewalls up and down

4 结 论

（1）超窄间隙焊接时对电弧加以有效约束，是防止电弧攀升和保证电弧在间隙两侧壁及其底部三个方向有效加热的可靠途径。

（2）增加焊接电流和送带速度，可使电弧的加热位置下移，电弧直接加热侧壁的高度减小，以至电弧能量密度提高，更有利于电弧对侧壁根部的加热；增加电弧电压，可使电弧阴极斑点的活动范围扩大，有利于增强弧柱和阴极斑点对侧壁根部的加热效果。

（3）电弧形态是决定侧壁熔合的主要因素，电弧电压、焊接电流和送带速度三者间的合理匹配，有利于获得合适的电弧形态，保证电弧在间隙的三个方向有效加热。

参考文献：

[1] Zhang Fuju，Xu Weigang，Wang Yutao，*et al*. Effect of welding heat input on HAZ character in ultra－fine grain steel welding [J]. China Welding，2003，12(2)：122－127.

[2] Bang K S，Kim W Y. Estimation and prediction of HAZ softening in thermomechanically controlled－rolled and accelerated－cooled steel [J]. Welding Research，2002(8)：174－179.

[下转第 64 页]

之一。

上述焊缝图像的处理算法是利用语言 Visual C 6.0^{++} 编程实现的。程序流程见图 6,用于运行程序的电脑为赛扬 CPU,主频为 3.2 G,内存为 1.0 G,对大小为 669×617 像素的图像进行上述处理,所需时间为 58 ms,能够满足实时跟踪的要求。

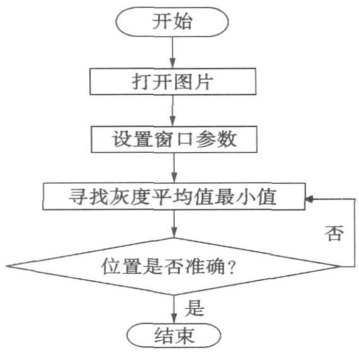

图 6 图像处理程序流程图

Fig. 6 Image processing flowchart

4 结 论

(1) 基于焊缝跟踪的轨道车辆塞拉门机器人焊接技术的应用使塞拉门制造技术达到国内领先水平。

(2) 在多条间断焊缝分组焊接的情况下,塞拉门机器人焊接可以采用每组焊接前进行焊缝跟踪的间歇式跟踪方式。

(3) 在非焊接情况下进行焊缝跟踪要配以适当的辅助光源,并要避免周围环境的强光等噪声对跟踪过程的干扰。同时,要采用适当分辨率的摄像机和视频采集卡,且摄像机以一定距离正对焊缝周围区域的表面采集图像。

(4) 对原始塞拉门框焊缝图像采用了传统的灰度变换、中值滤波、阈值变换、区域生长变换、细化变换一系列处理,该方法提取出的焊缝中心位置信息,适应性和抗干扰能力差,且有时无法正确计算焊缝中心位置。

(5) 移动窗口法能够弥补传统焊缝处理方法的诸多缺点,抗干扰能力强,能准确计算出当前焊缝与标准位置的偏差,速度快,满足实时跟踪要求。

参考文献:

[1] 刘极峰, 陈 旋, 李 超. 城轨门焊接机器人工作站技术经济分析[J]. 焊接技术, 2006(4): 57—59.

[2] 刘极峰, 闫 华, 毕光明. 塞拉门弧焊机器人工作站的研究[J]. 机电产品开发与创新, 2004, 17(5): 15—17.

[3] 邵秋萍, 刘极峰. 基于外部轴控制的塞拉门机器人弧焊工作站[J]. 机械设计与制造, 2006(9): 117—120.

[4] 刘极峰, 陈永胜, 邵秋萍, 等. 机器人技术基础[M]. 北京: 高等教育出版社, 2007.

[5] 刘极峰, 邱胜海, 王孜凌. 塞拉门弧焊机器人工作站柔性焊接夹具设计[J]. 机械设计与制造, 2005(5): 97—99.

[6] Bae K Y, Lee T H, Ahn K C. An optical sensing system for seam tracking and weld pool control in gas metal arc welding of steel pope [J]. Journal of Materials Processing Technolgy, 2002, 120(3): 458—465.

[7] Lee S, Chung S. A comparative performance study of several global thresholding techniques for segmentation[J]. Computer Vision, Graphics and Image Processing, 1990, 52(2): 171—190.

[8] Ostu N A. Threshold selection method from gray-level histograms[J]. IEEE Trams ON System Man and Cybernetics, 1979, 9(1): 62—66.

[9] Hsing Chia Kuo, Li Jen Wu. An image tracking system for welded seams using fuzzy logic[J]. Journal of Materials Processing Technology, 2002, 120(5): 169—185.

[10] 李嘉程, 彭天强, 彭 波, 等. 智能图像处理技术[M]. 北京: 电子工业出版社, 2003.

[11] Hewer G A, Kenney C, Manjunath B S. Variational image segmentation using boundary functions[J]. IEEE Transactions on Image Processing, 1998, 7(9): 1269—1282.

作者简介: 刘极峰, 男, 1955 年出生, 教授, 黄河科技学院特聘客座教授。主要从事机电工程方面的科研和教学工作。发表论文 60 余篇。

Email: liujf2002@163.com

[上接第 60 页]

[3] Zhu Liang, Zheng Shaoxian, Chen Jianhong. Development of ultra—narrow gap welding with constrained arc by flux band[J]. China Welding, 2006, 15(2): 44—49.

[4] 郑韶先, 朱 亮, 张旭磊, 等. 焊剂带约束电弧特性的试验分析[J]. 焊接学报, 2007, 28(8): 57—61.

[5] Nakamura T, Hiraoka K. Ultranarrow GMAW process with newly developed wire melting control system[J]. Science and Technology of Welding and Joining, 2001, 6(6): 355—362.

[6] 吴启东. 钨极焊接电弧在窄间隙中的电场分布[J]. 焊接学报, 1983, 4(1): 39—54.

作者简介: 郑韶先, 男, 1978 年出生, 博士研究生。主要从事焊接工艺及电弧物理的研究。发表论文 5 篇。

Email: zhengxian1115@lut.cn

factured by electron beam welding is simulated by finite element method, according to the relation between the power and weld depth, the heat input is decreased by change of the power with weld depth to control the welding distortion of blisk. The result of calculations shows that the blisk distortion of the aero-engine can be controlled by decreasing the heat input on the conditions of meeting the demand of weld penetration and guaranteeing the quality of the welding, a theoretical method and numerical data is provided for controlling the welding distortion of the aero-engine.

Key words: heat input; numerical simulation; distortion

Heat input mechanics for spot welding electrode based on FEM LUO Aihui[1], ZHANG Yansong[1], CHEN Guanlong[1], ZHU Wenfeng[2] (1. Mechanical and Power Engineering College, Shanghai Jiaotong University, Shanghai 200240, China; 2. Mechanical Engineering College, Tongji University, Shanghai 200092, China). p41—44

Abstract: In order to study the heat dissipation of electrode during the spot welding process, the heat input mechanics of electrode for spot welding was analyzed in detail firstly. Then, the heat input model for electrode was built based on the finite element method (FEM) and the information of heat input during the welding process was analyzed. Finally, experiment was carried out to validate the conclusion. It's found that the dissipating heat of electrode was made of resistance heat and conduction heat. The resistance heat had the same law with the welding current and the conduction heat was the major part of the dissipating heat. This research is helpful to the further study on heat dissipation of electrode and quality control of spot welding.

Key words: resistance spot welding; heat input; finite element method

Fatigue life analysis of lap-shear spot weld of dual phase steels XU Jun, ZHANG Yansong, ZHU Ping, CHEN Guanlong (Body Manufacturing and Technology Center, Shanghai Jiaotong University, Shanghai 200240, China). p45—48

Abstract: Dual phase steel spot weld characteristic was investigated. And then fatigue strength of dual phase steel lap-shear spot weld was tested, the data for spot weld fatigue curve were obtained. The fatigue crack propagation path and failure modes of specimens were also studied. On the basis of crack propagation path local equivalent stress intensity factor k_{eq} was applied to analyze the fatigue life of dual phase steel spot weld. The test result indicated that k_{eq} was an effective parameter to predict spot weld fatigue strength prediction, which can correlate fatigue life of spot weld specimens with different thickness and weld nugget size.

Key words: dual phase steels; spot welding; fatigue strength; local equivalent stress intensity factor

Analysis on arc spectral radiation of TIG welding process of steel and aluminum with different parameters LI Zhiyong[1], WANG Bao[1], LI Huan[2], YANG Lijun[2] (1. Welding Research Center, North University of China, Taiyuan 030051, China; 2. School of Materials Science and Engineering, Tianjin University, Tianjin 300072, China). p49—52, 56

Abstract: Through adjusting welding parameters such as welding current, arc length and gas flow rate, the spectral distributions of TIG welding arc were collected. In order to explore the variation of arc radiation in different spectral zone, TIG welding processes of steel and aluminum were studied for spectral distribution analysis, respeetively. For TIG welding of steel, the light radiation increases with the arc length in different spectral zone, among which the radiation intensity in spectral zones with less line spectrum increase linearly with the arc length. However, the change law is different for long arc and short arc. The light radiation increases with the growth of welding current. The light radiation is nearly the same when the gas flow rate was in a rather large value. When the gas flow rate was low which can not provide enough protection for the welding arc, the light radiation is affected obviously. For TIG welding of aluminum, the light radiation does not change a lot with the arc length variation. The radiation increases with the growth of welding current. The gas flow rate has great effect on the light radiation of arc when it is low, while has less effect on the light radiation of arc when it is high.

Key word: arc spectrum; welding parameter; TIG welding; intensity of radiation

Thermal cycling of rectangular chip resistor joints soldered with lead-free solder by diode laser HAN Zongjie[1], XUE Songbai[1], WANG Jianxin[1], YU Shenglin[1,2], FEI Xiaojian[1,3], ZHANG Liang[1] (1. College of Materials Science and Technology, Nanjing University of Aeronautics and Astronautics, Nanjing 210016, China; 2. The 14th Research Institute, China Electronics Technology Group Corporation, Nanjing 210013, China; 3. Guangzhou CSSC-Ocean-Gws Marine Engineering Co., Ltd., Guangzhou 510727, China). p53—56

Abstract: Soldering experiments of rectangular chip resistor components were carried out with Sn—Ag—Cu lead-free solder by diode laser soldering system and IR reflow soldering method, respectively, and the thermal cycling test of chip resistor component joints was also carried out. It is found that mechanical properties of chip resistor joints soldered by laser soldering system are better than the ones of chip resistor joints soldered by IR reflow soldering method; shear forces of chip resistor joints decrease gradually with the increasing of thermal cycling times, while at the same time, shear forces of laser soldered joints are larger than that of IR soldered joints. Shear fracture mode of chip resistor joints change from toughness fracture to brittle fracture as thermal cycling times increase.

Key words: rectangular chip resistor; Sn—Ag—Cu lead-free joints; diode laser soldering; thermal cycling

Heating characteristic of constricting arc with flux strips in ultra-narrow gap welding ZHENG Shaoxian, ZHU Liang, ZHANG Xulei, CHEN Jianhong (State Key Laboratory of Gansu Advanced Non-ferrous Metal Materials, Lanzhou University of Technology, Lanzhou 730050, China). p57—60, 64

Abstract: Constricting arc with flux strips is employed in ultra-narrow gap welding, by measuring the cross sectional sizes of welds under different welding parameters, heating characteristic of

constricted arc was analyzed based on the variation of the cross sectional sizes of welds. The results indicate the arc with effective constriction in the ultra-narrow gap benefits from preventing itself climbing up along sidewalls, and ensure a reliable fusion of sidewalls; arc morphology is the main factor to decide fusion of sidewalls, the increase of welding current or feeding rate of flux strip can make the heating position of arc move down, the heating height of sidewalls decrease, energy density of arc enhance, which more benefits from achiving good fusion of sidewall roots; the increase of voltage can make the range of cathode spot moving expand, which can enhance the heating effect of arc column and cathode spot on sidewall roots; the reasonable matching of voltage, current and feeding rate of flux strip is good to obtain proper arc morphology, and makes arc have a effective heating in three directions of ultra-narrow gap.

Key words: constricting arc with flux strips; ultra-narrow gap welding; heating characteristic

An image processing method for vision tracking of sliding door seam LIU Jifeng[1], XIAO Zengwen[1], ZOU Jingchao[2], YANG Xiaolan[3] (1. College of Mechanical Engineering, Nanjing Institute of Technology, Nanjing 210013, China; 2. College of Engineering, Huanghe S & T University, Zhengzhou 450015, China; 3. College of Material Engineering, Nanjing Institute of Technology, Nanjing 210013, China). p61—64

Abstract: With the rapid development of city railroad vehicles and bullet train, the automatic welding technology should be improved instantly. Welds are numerous and short in sliding door and welding should be high quality and exact, so a vision tracking system of discontinuous robot arc welding with normal lamp-house was produced. A series of processes of vision tracking image with normal lamp-house were established, which is the image processing technologies that gray-scale transform, median filter, image segmentation, etc. Traditional image segmentation includes gray-scale transform and line thinning, etc. They seam position can be found by its sides. However, the result by this method is easily disturbed by noises such as dark or bright cutter traces, and so on. A movable window technology was produced. This technology takes the position, which the average gray scale of all the pixels in a window is the minimum one, as the current position. And the window has the same size and shape as the seam and can be moved through the acquired image. The technology takes the whole pixels of the seam as the calculating data. As a result, it is powerful anti-jamming and can effectively filter the noises of the dark and bright cutter traces. The error of the seam position can be directly calculated after the current and standard positions are compared. The actualizing steps of movable window technology are also presented. The tests at arc welding robot workstation for the sliding door show that the seam image processing system has powerful adaptability and anti-jamming ability. And its fast work speed can meet the request of real time tracking.

Key words: sliding door; arc welding robot; seam tracking; image process; movable window

Structure and abradability of Cu—Al_2O_3 gradient coatings fabricated by plasma spraying LEI Ali, LI Gaohong, FENG Lajun, DONG Nan (School of Materials Science and Engineering, Xi' an University of Technology, Xi' an 710048, China). p65—68

Abstract: In reflection to the fact that the low adhesion strength and high porosity affected the coatings' abradability of pure ceramic coatings, Cu—Al_2O_3 gradient coatings were fabricated by plasma spraying. The methods of SEM, metallurgical microscope and so on were used to analyse microstructure and component of the coatings and self-made mounting grinding abrasion probe aircraft was used to measure the wearing grinding abrasion of Cu—Al_2O_3 gradient coatings. The results showed that the Cu—Al_2O_3 gradient coatings fabricated by plasma spraying have not apparent structure-accident and macrography interlamination interface, and the structure of coatings express the features of non-homogeneous in macrography and continuous in microscopic. The abradability of coatings is highest when the content of Al_2O_3 in gradient coatings reaches 80%, which is triple of base body. As the content of Al_2O_3 continues enlarging to pure ceramic coatings, its abradability falls down.

Key words: plasma spraying; Al_2O_3 ceramics; gradient coatings; grinding abrasion

Numerical simulation of influence of process on stress field of electron beam brazing radiator LI Junmin, CHEN Furong (College of Materials Science and Engineering, Inner Mongolia University of Technology, Hohhot, 010051, China). p69—72

Abstract: The measurement of residual stress of electron beam brazing (EBB) is difficult, so a two-dimonsional FEM model was established to simulate the residual stress field by ANSYS softwane. And the influences of two kinds of process on residual stress of 1Cr18Ni9Ti stainless steel radiator joint of EBB were analyzed to optimize the process and parameters. The results show that, for radial residual stress, the obvious stress concentration region was found in faying face by direct-heating process; while there was no stress concentration in faying face by stage-by-stage heating process; For circumferential residual stress, conpared the stage-by-stage heating process with direct-heating process, the peak value of tensile stress reduces by 11.2%. Compared circumferential residual stress with radial residual stress by two kinds of brazing process, the peak value of circumferential tensile stress is higher than that of radial tensile stress. So the dangerous position of faying face is along circle direction, namely, the heating direction of scanning electron beam.

Key words: electron beam brazing; residual stress; numerical simulation

Thermal mechanical coupling analysis on initial period of FHPP in friction stitch welding ZHANG Baosheng, JIAO Xiangdong, CHEN Jiaqing, ZHOU Canfeng (Research Center of Offshore Engineering Joining Technology, Beijing Institute of Petrochemical Technology, Beijing 102617, China). p73—76, 80

Abstract: The fundamental forming process of friction stitch welding is friction hydro pillar processing, which is the key process that effects the quality of Friction Stitch Welding. A three-dimensional thermal mechanical coupling model of FHPP process was established by using finite element code MSC. Marc. The calculated